

Technical Note: Comparison of radiometric techniques for estimating recent organic carbon sequestration rates in temperate inland wetland soils

Purbasha Mistry¹, Irena F. Creed^{1,2}, Charles G. Trick³, Eric Enanga², David A. Lobb⁴

¹ School of Environment and Sustainability, University of Saskatchewan, 117 Science Place, Saskatoon, SK, S7N 5C8, Canada

² Department of Physical and Environmental Sciences, University of Toronto, 1265 Military Trail, Toronto, ON, M1C 1A4, Canada

³ Department of Health and Society, University of Toronto, 1265 Military Trail, Toronto, ON, M1C 1A4, Canada

⁴ Department of Soil Science, University of Manitoba, 13 Freedman Crescent, Winnipeg, MB, R3T 2N2, Canada

Correspondence to: Irena F. Creed (irena.creed@utoronto.ca)

Abstract. For wetlands to serve as natural climate solutions, accurate estimates of organic carbon (OC) sequestration rates in wetland sediments are needed. Dating using cesium-137 (¹³⁷Cs) and lead-210 (²¹⁰Pb) radioisotopes is commonly used for measuring OC sequestration rates in wetland sediments. ¹³⁷Cs radioisotope dating is relatively simple, with calculations based on a single point representing the onset (1954) or peak (1963) of the ¹³⁷Cs fallout. ²¹⁰Pb radioisotope dating is more complex as the calculations are based on multiple points. Here, we show that reliable dating of sediment cores collected from wetlands can be achieved using either ¹³⁷Cs or ²¹⁰Pb dating or their combination. However, ¹³⁷Cs and ²¹⁰Pb profiles along the depth of sediment cores need to be screened, analyzed, and interpreted carefully to estimate OC sequestration rates with high precision. To this end, we propose a decision framework for screening ¹³⁷Cs and ²¹⁰Pb profiles into high- and low-quality sediment profiles, and we compare dating using the 1954 and 1963 time-markers, i.e., the rates of sedimentation and, consequently, OC sequestration over the past ~60 years. Our findings suggest that ¹³⁷Cs- and ²¹⁰Pb-based OC sequestration rates are comparable, especially when using the 1963 (vs. 1954) time-marker.

1 Introduction

Wetlands in agricultural landscapes serve a crucial role in providing habitat for wildlife, regulating climate, improving water quality, and reducing floods. Moreover, these wetlands have the potential to sequester organic carbon (OC) (Bridgman et al., 2006; Nahlik and Fennessey, 2016; Bansal et al., 2023). Accounting for the balance between the sequestration and emission of carbon can help establish wetlands as essential candidates for natural climate solutions by offsetting carbon emissions (Hambäck et al., 2023). These wetlands embedded in agricultural landscapes are recognized as temperate inland wetland soils. The global carbon stock of temperate inland wetland soils is estimated to be 46 Pg C to 2 m depth, and Canada's

29 temperate inland wetland soils are estimated to contain 4.6 Pg C (Bridgham et al., 2006). Compared to peatlands, the rapid
30 rate of OC sequestration and the more considerable spatial extent of temperate inland wetland soils can help contribute
31 significantly to regional or national carbon sequestration (Bridgham et al., 2006; Nahlik and Fennessey, 2016).

32

33 Canada encompasses around 25% of the world's wetlands, with an area of approximately 1.29 million square kilometers,
34 which accounts for 13% of the country's terrestrial area (Environment and Climate Change Canada, 2016), highlighting the
35 global importance of these wetlands. Unfortunately, there is minimal data on the OC sequestration rates in these wetlands.
36 To estimate the OC sequestration potential of these wetlands, it is essential to establish precise measurements to quantify
37 wetland OC sequestration, develop strategies to promote conservation and restoration efforts, incorporate carbon credits in
38 the carbon markets, and validate the wetland-based ecosystem services.

39

40 There are several ways to estimate the potential of wetlands to store OC (Bansal et al., 2023). One of these methods is
41 radiometric dating, which can calculate the OC storage rates of wetlands over periods of 10 to $\geq 1,000$ years. Frequently used
42 radioisotopes for radiometric dating are cesium-137 (^{137}Cs) and lead-210 (^{210}Pb), which can be used to estimate relatively
43 recent (up to the last 100 years) OC sequestration rates (Villa and Bernal, 2018). Estimating OC sequestration rates involves
44 building an age-depth profile or model of ^{137}Cs and ^{210}Pb from sediment cores that demonstrate the relationship between the
45 depth of sediment layers and their corresponding age. Since the inorganic radioisotopes (^{137}Cs and ^{210}Pb) strongly bind with
46 the soil particles once in contact, the radioisotopes can act as an efficient tracer for investigating OC sequestration rates
47 (Ritchie and McHenry, 1990; Craft and Casey, 2000). These characteristics allow for accurate tracking of carbon movement
48 within ecosystems, thereby enabling the extraction of detailed information about carbon sequestration dynamics in wetlands.

49

50 The characteristics of ^{137}Cs and ^{210}Pb to estimate wetland OC sequestration rates are presented in Table 1. ^{137}Cs is an
51 artificial radioisotope that was produced during thermonuclear bomb testing in the 1950s and 1960s, with the onset of
52 atmospheric deposition in 1954 and a peak in 1963 (Ritchie and McHenry, 1990). The testing caused radioactive uranium to
53 decay, and, as a result, ^{137}Cs isotope was released into the atmosphere, which was then deposited around the globe. Although
54 there may be challenges in applying our study to some parts of the world, the information is generally applicable and
55 valuable for consideration in all regions. We encourage others to customize this approach further for use in other regions
56 where Cs deposition histories vary.

57

58 ^{137}Cs has a half-life of 30.17 years, which can be used to estimate the last ~50-70 years of OC sequestration rates in wetlands
59 (e.g., Bernal and Mitsch, 2012). ^{137}Cs dating assumes constant sedimentation rates measured since 1954 or 1963. In using the
60 two time-markers for ^{137}Cs , we do not expect the sedimentation rates to be equal, but we do expect them to be similar. The

61 onset and the peak of ^{137}Cs activity at 661.6 keV can be used to mark 1954 and 1963, respectively. These time-markers
62 (1954 and 1963) can date sediment layers (Pennington et al., 1973; Ritchie and McHenry, 1990; DeLaune et al., 2003) and
63 consequently the OC sequestration rates. ^{137}Cs has an additional time-marker for Europe in 1986 due to the Chernobyl
64 nuclear accident and for Japan in 2011 due to the Fukushima Daiichi nuclear accident (Foucher et al., 2021), indicating that
65 OC sequestration estimates can be derived for different timescales. In the Americas, we do not see evidence of the 1986 or
66 2011 ^{137}Cs peak, which is observed in Europe and Japan, respectively, so we did not need to use other radioisotope
67 techniques (e.g., $^{239+240}\text{Pu}$) to distinguish the 1986 or 2011 ^{137}Cs peak from the 1963 ^{137}Cs peak. ^{137}Cs dating requires a
68 gamma spectrometer to estimate OC sequestration rates. Sample preparation for gamma analysis involves drying, weighing,
69 disaggregating, homogenizing, and sieving (Bansal et al., 2023). Samples vary from 1 to 1,500 g, with smaller samples
70 associated with higher uncertainties and, therefore, requiring longer times to analyze. Gamma analysis counting times range
71 from 4 to 48 h for each sample (e.g., 4 to 12 h in Li et al., 2007; 12 to 24 h in Zarrinabadi et al., 2023; and 24 to 48 h in
72 Kamula et al., 2017). ^{137}Cs dating provides a simple result (an average sedimentation rate), while ^{210}Pb dating provides a
73 more complex result (using a supply rate model to reveal trends in sedimentation rates). Plutonium (Pu) may replace ^{137}Cs in
74 the future due to concerns of half-life and persistence as a dating tool. In essence, $^{239+240}\text{Pu}$ has the same source and
75 deposition mechanism as ^{137}Cs . Its longer half-life will make its peak measurable when ^{137}Cs is no longer measurable.

76

77 Unlike ^{137}Cs , ^{210}Pb is a naturally occurring radionuclide derived from ^{238}U and deposits atmospherically from the decay of
78 radium-226 (^{226}Ra) (Walling and He, 1999). ^{210}Pb has a half-life of 22.3 years and is used to estimate the last 10-150 years of
79 OC sequestration rates in wetlands (Craft and Richardson, 1998; Craft and Casey, 2000; Craft et al., 2018; Creed et al.,
80 2022). ^{210}Pb activity can be measured using gamma (observed at 46.5 keV) and alpha spectrometry (destructive) (Walling
81 and He, 1999; Bellucci et al., 2007). Traditional alpha analysis requires 0.2-0.5 g of sample and additional sample
82 preparation involving leaching with hydrochloric and nitric acid and electroplating (up to 24 h for sample preparation)
83 (Bansal et al., 2023). Alpha analysis can be considered an indirect method for ^{210}Pb dating where polonium-210 (^{210}Po)
84 activity is measured, assuming both ^{210}Pb and ^{210}Po are in a secular equilibrium. ^{210}Pb activity is calculated by comparing
85 ^{210}Po activity against the known activity of ^{209}Po (isotope tracer). In alpha analysis, the additional time required for sample
86 preparation is compensated by running multiple samples simultaneously (Bansal et al., 2023). Gamma and alpha
87 spectrometry of ^{210}Pb provides the total ^{210}Pb activity, which incorporates unsupported (or excess) ^{210}Pb ($^{210}\text{Pb}_{\text{ex}}$) and
88 supported ^{210}Pb . $^{210}\text{Pb}_{\text{ex}}$ is used to determine the mass or sediment accumulation rate. Supported ^{210}Pb is derived from the
89 natural decay of ^{226}Ra in the sediment, while unsupported ^{210}Pb comes from the decay of atmospheric radon-222 (^{222}Rn),
90 which deposits ^{210}Pb onto the sediment surface from the air. Unsupported ^{210}Pb activity decreases over time due to
91 radioactive decay, unlike supported ^{210}Pb (Appleby and Oldfieldz, 1983). The choice of model used in ^{210}Pb dating can
92 reflect constant and variable sedimentation rates (Sanchez-Cabeza and Ruiz-Fernandez, 2012) and, consequently, OC

93 sequestration rates in wetlands. Some models used for ^{210}Pb dating are (1) constant flux-constant sedimentation (CFCS)
94 model, (2) constant rate of supply (CRS) model, and (3) constant initial concentration (CIC) model (Appleby and Oldfield,
95 1978). Both ^{137}Cs and ^{210}Pb provide suitable time-markers and a longer time horizon compared to direct measurements using
96 the time-marker of horizons (2-10 years) to study sediment accretion and, subsequently, OC sequestration rates in wetlands
97 (Bernal and Mitsch, 2013; Villa and Bernal, 2018). In this study, we compared the average OC sequestration rate derived
98 from ^{137}Cs temporal markers with the progressive OC sequestration rates derived using a constant rate of supply model
99 applied to ^{210}Pb .

Table 1: Characteristics of ^{137}Cs and unsupported ^{210}Pb ($^{210}\text{Pb}_{\text{ex}}$) dating to estimate sedimentation rates in wetlands.

| Method of radiometric dating | ^{137}Cs | $^{210}\text{Pb}_{\text{ex}}$ |
|---|--|---|
| Type of radioisotope | Artificial (atmospheric deposition 1954 – 1963). | Natural. |
| Half life | 30.17 years. | 22.3 years. |
| Time-marker | 1954 (onset) and 1963 (peak). | Recent (10-20 years) to a maximum of 50-150 years. |
| Radiometric Technique | Gamma spectrometry (nondestructive). | Gamma (nondestructive) and alpha spectrometry (destructive). |
| Pre-processing | Drying, weighing, disaggregating, homogenizing, and sieving. | For gamma analysis, drying, weighing, disaggregating, homogenizing, and sieving prior to analysis on a gamma counter. For alpha analysis, leaching with hydrochloric and nitric acid and electroplating of ^{210}Po which constitutes allowing the digested and therefore extracted ^{210}Po isotope solution to settle on silver coins overnight before measuring the ^{210}Po (known tracer) and ^{210}Po activity (sample) next morning through the alpha counter/ensemble. |
| Sample size | Minimum 1 g (larger sample size has higher certainty). | 1 to 5 g for gamma spectrometry, 0.2 to 0.5 g for alpha spectrometry. |
| Time requirement for radiometric dating | 48 h for each sample for gamma spectrometry. | 48 h for each sample for gamma spectrometry. 48 to 72 h for multiple samples plus sample preparation time per multiple samples. |
| Output | A single average sedimentation rate. | Variable sedimentation rate. |
| Estimation approach | Onset of ^{137}Cs activity represents 1954 and highest peak of ^{137}Cs activity represents 1963, observed at 661.6 keV. | Activity of ^{210}Pb is observed at 46.5 keV. Excess ^{210}Pb is used to determine the vertical accretion. |
| Complexity in estimation | Simple; estimated by using time-marker of onset or peak ^{137}Cs activity and associated sediment accumulation. | More complex; estimated by one of several models to estimate sedimentation rate. Most common models are (1) constant flux–constant sedimentation model, (2) constant rate of supply model, and (3) constant initial concentration model (Appleby and Oldfield, 1978) |

101

102 The combined use of ^{137}Cs and ^{210}Pb may improve the accuracy of the dating estimation (Drexler et al., 2018; Creed et al.,
103 2022). The more detailed assessment accrues a higher cost and time requirement, and the need for specialized equipment and
104 technical expertise to conduct laboratory and data analyses may constrain the research efforts (Bansal et al., 2023).
105 Furthermore, factors such as timescales, analytical complexity in interpreting radioisotope profiles (e.g., ^{137}Cs peak clarity),
106 variability in atmospheric deposition, and mobilization of radioisotopes can contribute to uncertainty (Drexler et al., 2018;
107 Loder and Finkelstein, 2020; Zhang et al., 2021; Bansal et al., 2023) and limit the applicability of one radioisotope over the

108 other. Therefore, it is essential to consider the advantages and potential challenges of using radioisotopes before designing
109 research studies.

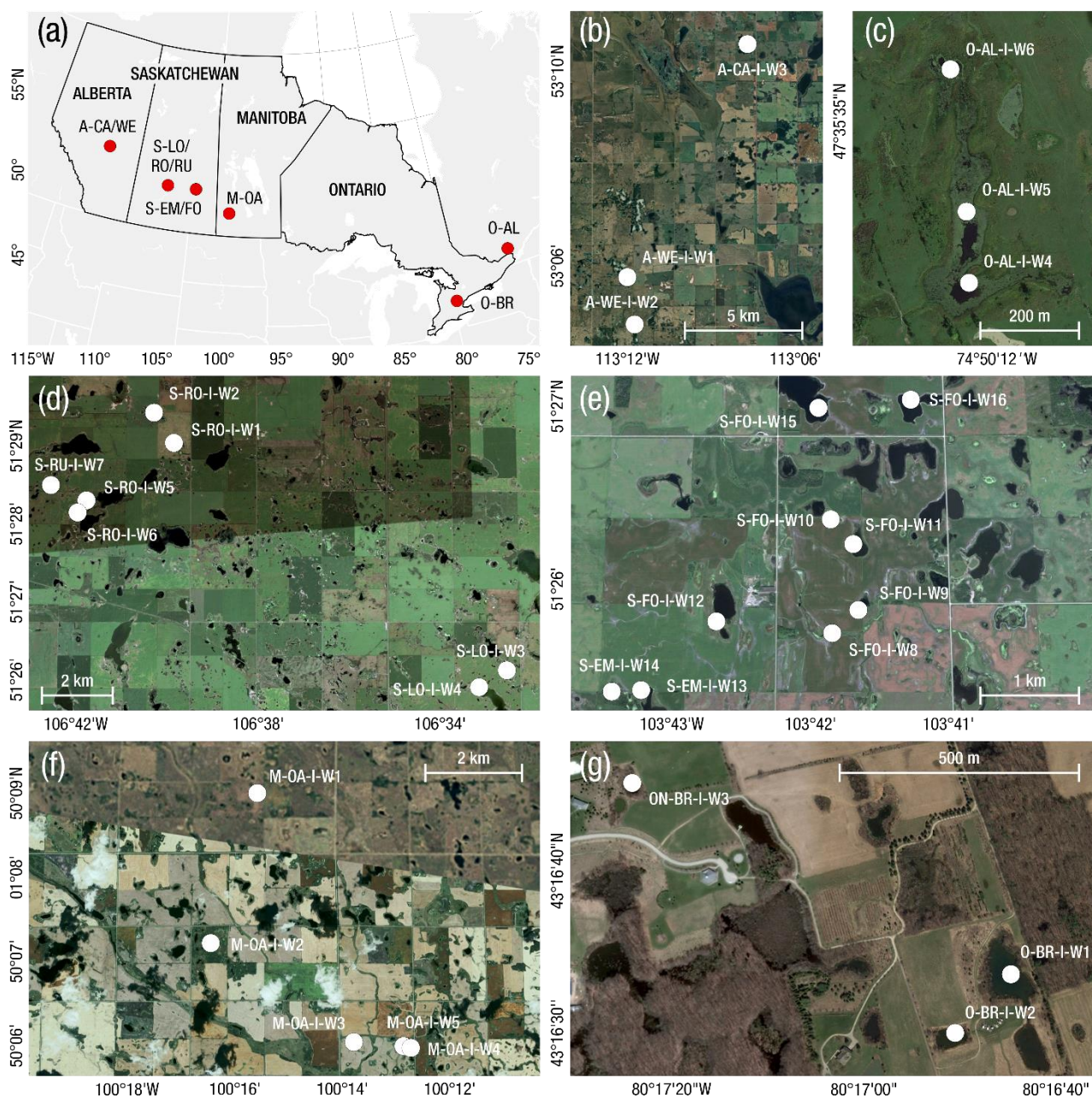
110

111 The main objective of this research paper is to explore the use of ^{137}Cs and ^{210}Pb to estimate recent OC sequestration rates in
112 undisturbed (i.e., not directly impaired by human activities) temperate inland wetland soils located on agricultural
113 landscapes. Here, we aim to (1) categorize ^{137}Cs or ^{210}Pb profiles into high- and low-quality via a decision framework, (2)
114 apply the decision framework to estimate OC sequestration rates, (3) use 1963 and 1954 time-markers to compare the ^{137}Cs -
115 and ^{210}Pb -based OC sequestration rates to get a better understanding of the sediment history, and (4) select the best approach
116 for ^{137}Cs and ^{210}Pb to estimate the OC sequestration rates with highest precision. This study helps reduce uncertainty in
117 studies that rely on ^{137}Cs or ^{210}Pb radioisotope dating.

118 **2 Methods**

119 **2.1 Sediment core collection**

120 Triplicate sediment cores were collected from 30 undisturbed temperate inland wetland soils in agricultural landscapes
121 across southern Canada (Fig. 1). A summary of the physical characteristics of these wetlands can be found in Supplementary
122 Table 1. These wetlands were undisturbed, with no known history of cultivation. The sediment cores were extracted from the
123 center of the wetland, constituting the open-water area. A Watermark Universal Corer (inner diameter of 6.8 cm) or
124 VibeCore Mini with poly core tubes (inner diameter of 7.6 cm) were used to collect most of the sediment cores. A JMP
125 BackSaver Soil sampler (inner diameter of 3.8 cm) was used for compacted sediment cores. Shallow (15 to 90 cm) sediment
126 cores were sectioned into 1- or 2-cm increments. Deeper (> 90 cm) sediment cores were sectioned into 5-cm increments. The
127 sediment cores were stored at -5 °C for further processing at the laboratory.



128

129

130

131

132

133

Figure 1: (a) Study area situated in four provinces of Canada; (b) three wetland sites in Alberta (AB); (c) three wetland sites in Ontario (ON); (d) seven wetland sites in Saskatchewan (SK); (e) nine wetland sites in Saskatchewan (SK); (f) five wetland sites in Manitoba (MB); and (g) three wetland sites in Ontario (ON). Figures (b)-(g) are based on the sampling locations of wetlands used in this study reproduced using Google Earth Images [(b) and (c) ©2024 Airbus; (d), (e), and (g) ©2024 Maxar Technologies; (f) ©2024 Airbus and Maxar Technologies].

134 **2.2 Generation of ^{137}Cs and ^{210}Pb profiles**

135 Sediment core increments were weighed (wet mass), dried, weighed again (dry mass), disaggregated, homogenized, and
136 sieved. The increments were sieved to remove gravel (> 2 mm); radioisotopes do not bind on the gravel, and gravel does not
137 contain OC; therefore, eliminating gravel improves the estimate of radioisotopes and OC. The increments were counted at
138 661.6 keV for ^{137}Cs activity and 46.5 keV for ^{210}Pb activity. ^{137}Cs analysis was performed using a gamma spectrometer, and
139 ^{210}Pb analysis was performed using both gamma and alpha spectrometers to increase throughput rates. The gamma analysis
140 was conducted using the high-purity germanium detectors; e.g., Broad Energy Germanium detectors (BE6530) and Small
141 Anode Germanium well detectors (GSW275L) (Mirion Technologies, Inc., Atlanta, GA, USA). The alpha analysis was
142 conducted using ORTEC® alpha spectrometer (AMETEK® Advanced Measurement Technology, TN, USA). Both
143 radioisotope analyses were performed at the Landscape Dynamics Laboratory, University of Manitoba, Winnipeg, Canada.
144 Although the underlying principles of gamma and alpha analysis differ, each focuses on quantifying the decay of ^{210}Pb ,
145 generating comparable results (Zaborska et al., 2007). Measurement accuracy of gamma detectors is ensured by assessing the
146 counting errors with reference materials within the same geometry as the sample (e.g., petri dish). Detection error was < 10%
147 with a counting time of up to 24 h. Furthermore, Landscape Dynamics Laboratory undergoes regular Proficiency Testing
148 through the International Atomic Reference Material Agency (IARMA) and previously through the International Atomic
149 Energy Agency (IAEA) to ensure acceptable accuracy and precision of analytical results using gamma spectroscopy.

150 **2.3 Screening of ^{137}Cs and ^{210}Pb profiles**

151 Sediment cores were screened to remove profiles with evidence of vertical mixing, and then the remaining profiles were used
152 to estimate OC sequestration rates using ^{137}Cs or ^{210}Pb radioisotope dating. The actual ^{137}Cs peak can vary from the expected
153 peak, increasing uncertainty in ^{137}Cs dating (Drexler et al., 2018). ^{137}Cs peaks can be “noisy” or “disturbed”; i.e., flattened,
154 broadened, truncated, mixed, fluctuating (Drexler et al., 2018), or one-sided where the ^{137}Cs peaks appear at the surface of
155 the sediment core (indicating no or little sedimentation since 1963). The magnitude and shape of the ^{137}Cs peaks observed in
156 the sediments can be affected by the atmospheric deposition rate of ^{137}Cs , which is obviously affected by the number and
157 magnitude of emission events and the weather conditions following these events (UNSCEAR, 2000). The magnitude and
158 shape of these peaks are also impacted by the movement of water and sediment within each wetland's catchment during the
159 peaks' development (Milan et al., 1995; Zarrinabadi et al., 2023). Here, changes in the shape of the peaks are caused by the
160 upward and downward movement of the sediment within the sediment profile (the movement of ^{137}Cs through diffusion
161 (Klaminder et al., 2012) is presumed negligible). Bioturbation can cause an upward and downward mixing of the ^{137}Cs in the
162 profile, resulting in peak attenuation (Robbins et al., 1977). Even wave action during the period of atmospheric deposition
163 will have a similar attenuation effect (Andersen et al., 2000; Zarrinabadi et al., 2023). Following peak atmospheric
164 deposition, soil erosion and the accumulation of sediment will deliver sediments to the top of the profile, and those sediments

165 may be higher or lower in concentration depending on the degree of preferential sediment transport and the associated
166 enrichment or depletion of ^{137}Cs in the added sediment (Zarrinabadi et al., 2023). Such noise in ^{137}Cs peaks needs careful
167 interpretation to avoid over- or under-estimating the OC sequestration rates.

168
169 *Selecting suitable cores:* Of the 90 sediment cores (30 wetlands x 3 replicates = 90), 79 were suitable (complete and datable)
170 for ^{137}Cs dating and 47 for ^{210}Pb dating. Only some replicates from the same wetland were ideal for interpretation or further
171 screening. The suitability of ^{137}Cs profiles for dating was assessed by zero activity before the onset and peak of ^{137}Cs
172 activity. The suitability of ^{210}Pb profiles for dating was evaluated by determining the exponential decline in ^{210}Pb activity
173 with depth until background levels are reached.

174
175 *Classification of the selected ^{137}Cs profiles:* The 79 suitable ^{137}Cs profiles were then classified into high- and low-quality
176 using the following steps (Fig. 2a):

- 177
178 1. The ^{137}C depth profile and the shape of the peak were assessed. A clear and distinct peak associated with several
179 points on both sides of the peak verified the ^{137}Cs depth profile as high-quality (e.g., Fig. 3a).
- 180 2. When analyzing sediment samples, a clear peak in ^{137}Cs activity didn't always exist (e.g. Fig 4a). If a peak was
181 absent, which could have resulted from sediment influxes with very high or very low ^{137}Cs activity levels, the total
182 ^{137}Cs activity of the entire profile was examined. If the cumulative ^{137}Cs inventory value for the entire profile was \geq
183 500 Bq m^{-2} , then the ^{137}Cs profile was considered high-quality. Conversely, if the cumulative ^{137}Cs inventory value
184 for the entire profile was $< 500 \text{ Bq m}^{-2}$, the ^{137}Cs profile was considered low-quality. The cutoff cumulative ^{137}Cs
185 inventory value of 500 Bq m^{-2} was established by assessing the ^{137}Cs reference inventory value, the value of ^{137}Cs
186 present in a non-eroded system with an undisturbed profile. The ^{137}Cs reference inventory value differs from region
187 to region (Owens and Walling, 1996), and the most proximal regional value was used to select the cutoff ^{137}Cs
188 inventory value (Sutherland, 1991; Kachanoski and Von Bertoldi, 1996; Zarrinabadi et al., 2023). The ^{137}Cs
189 reference inventory is a catchment-wide reference value and not specific to the wetland center; thus, the cumulative
190 ^{137}Cs inventory value of 500 Bq m^{-2} was viewed as a conservative indicator of the suitability of the ^{137}Cs profiles.
191 Ideally, reference sites are large, open, level, non-eroded areas, usually in forage or grassland since the 1950s, and
192 within 10 km of the site of interest. In this study, it was impossible to identify a suitable reference site near every
193 wetland; it is usually difficult to find reference sites in agricultural landscapes. However, we could locate reference
194 sites used in other studies within 50 km except from nine wetlands in SK (51° N and 104° W), which were $\sim 150 \text{ km}$
195 from the reference site. Although this was not considered ideal, it was considered acceptable.

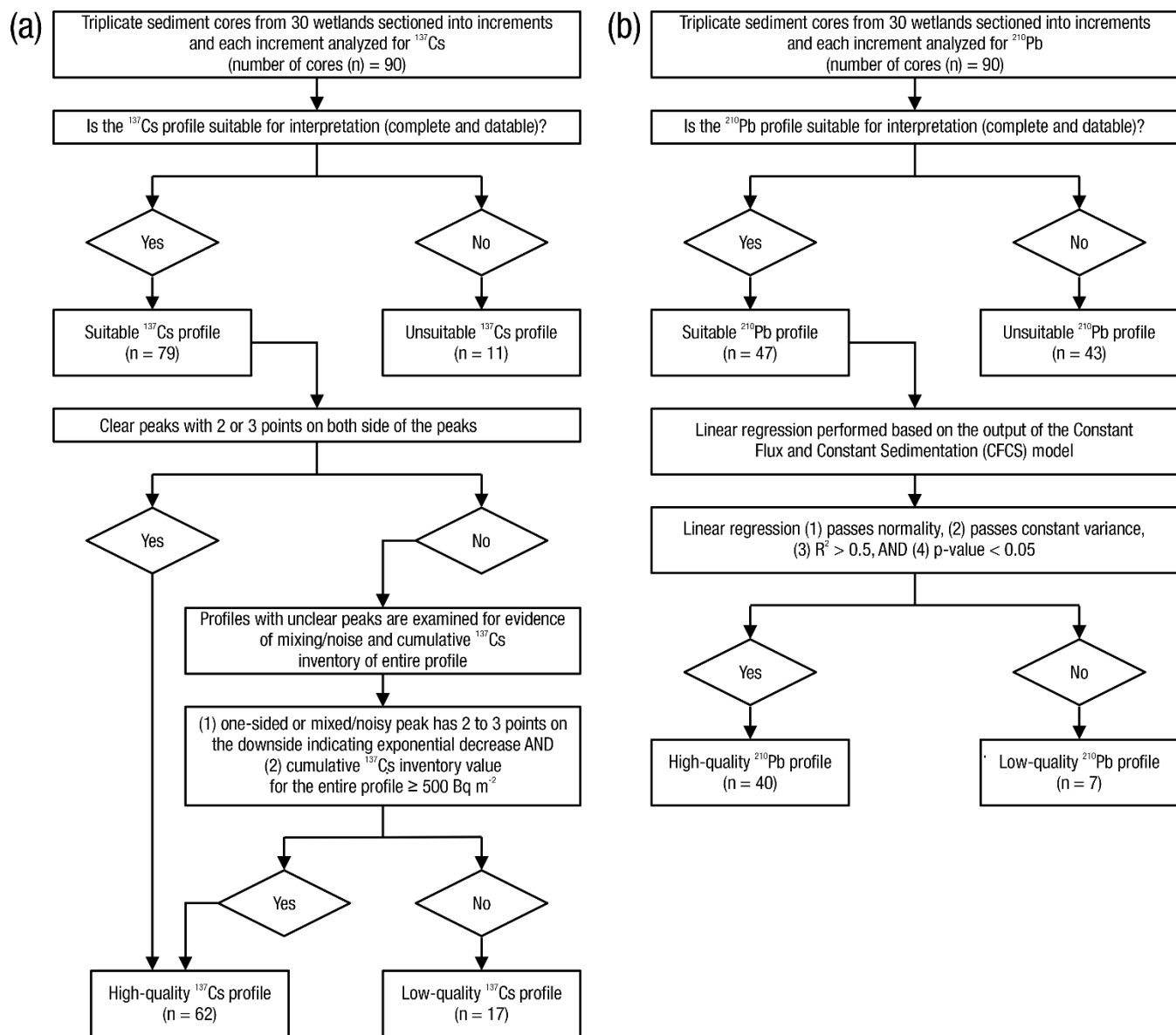
197 *Classification of the selected ^{210}Pb profiles:* The 47 suitable ^{210}Pb profiles were classified into high- and low-quality profiles
198 based on the following steps (Fig. 2b):

199

- 200 1. ^{210}Pb activity were plotted with a log-transformed $^{210}\text{Pb}_{\text{ex}}$ against mass depth (g cm^{-2}).
- 201 2. A linear regression analysis was performed (where the slope is used to derive the mass or sediment accumulation
202 rate in $\text{g cm}^{-2} \text{yr}^{-1}$).
- 203 3. If the linear regression passed both normality and constant variance tests and had an $R^2 > 0.5$ and a p-value < 0.05 ,
204 then the ^{210}Pb profile was classified as high-quality (e.g., Fig. 3a).
- 205 4. If either normality and constant variance tests were not passed, with an $R^2 \leq 0.5$ or a p-value ≥ 0.05 , then the ^{210}Pb
206 profile was considered low-quality (e.g., Fig. 3b).

207

208 The ^{210}Pb profiles were also classified using a two-step piecewise linear regression model to capture recent shifts in OC
209 sequestration rates. However, no significant improvement was observed. Consequently, ^{210}Pb -based OC sequestration rates
210 were derived from the linear regression line. An $R^2 > 0.5$ was selected as the cut-off for selecting high-quality over low-
211 quality profiles. Increasing the cut-off R^2 value may produce better profiles to be chosen for the study. Still, it can reduce the
212 number of available sediment cores and potentially ignore the natural variability and significant events occurring in the real
213 environment.



215

216

217

Figure 2: Classification of high- and low-quality ^{137}Cs and ^{210}Pb profiles outlining the decision frameworks for screening (a) ^{137}Cs and (b) ^{210}Pb profiles.

218 **2.4 Organic carbon stocks and sequestration rates**

219 Radioisotope activity measurements were utilized to assign two time-markers, one for 1954 and the other for 1963, in the
220 sediment cores. Sediment radioisotope dating was used to calculate the rates of sediment or mass accumulation and OC
221 sequestration.

222
223 For ^{137}Cs dating, sediment accumulation and OC sequestration rates ($\text{Mg ha}^{-1} \text{ yr}^{-1}$) were estimated using the cumulative sum
224 of sediment or OC (Mg ha^{-1}) from the surface to the depth corresponding to the time-markers of ^{137}Cs of each core and
225 dividing by the number of years from the time-marker to the years the samples were collected. Unit conversion is applied to
226 report the OC sequestration rate estimates in $\text{Mg ha}^{-1} \text{ yr}^{-1}$ from $\text{g cm}^{-2} \text{ yr}^{-1}$ for easy standardization and comparability with
227 other studies. For ^{137}Cs profiles with noisy peaks and comparatively larger cumulative ^{137}Cs inventory values, the first
228 elongated peak with a sharp rise after the onset of the ^{137}Cs peak was considered the 1963 peak instead of the peak with the
229 highest activity in the profile.

230
231 For ^{210}Pb dating, mass or sediment accumulation and OC sequestration rates were estimated using the Constant Flux and
232 Constant Sedimentation (CFCS) model (Sanchez-Cabeza and Ruiz-Fernandez, 2012; Kamula et al., 2017). Here, $^{210}\text{Pb}_{\text{ex}}$ was
233 estimated by subtracting ^{226}Ra activity (186 keV) from the total ^{210}Pb activity. The CFCS model uses the log-linear
234 relationship of $^{210}\text{Pb}_{\text{ex}}$ with mass depth and converts $^{210}\text{Pb}_{\text{ex}}$ to the mass or sediment accumulation rate and, consequently, the
235 OC sequestration rate. The OC stock was estimated by taking the cumulative sum of OC (Mg ha^{-1}) from the surface of each
236 sediment core to the depth increments represented by the time-marker (e.g., 1963).

237
238 OC stocks for the 1954 and 1963 time-markers were calculated by multiplying the OC content per unit mass of soil (g).
239 Here, OC content was calculated from OC concentration (%) measured by loss-on-ignition (LOI) method (Kolthoff and
240 Sandell, 1952) by the mass of sediment for each section interval and specific depth interval per unit area (g cm^{-2}) down the
241 profile to the respective time-marker. OC (%) was calculated by multiplying organic matter (%) by LOI with 0.58, assuming
242 58% of the organic matter is carbon. Despite the broad applicability, simplicity in measurement techniques, and cost-
243 effectiveness, the LOI approach is associated with some limitations, such as the ignition of non-organic particles at high
244 temperatures or the use of a conventional conversion factor (Pribyl, 2010; Hoogsteen et al., 2015), which can result in over-
245 estimation of OC content.

246 **2.5 Statistical analysis**

247 Statistical analyses used sediment cores with ^{137}Cs - and ^{210}Pb -based OC sequestration rates available (number of sediment
248 cores (n) = 44). The ^{137}Cs —and ^{210}Pb -based estimates of OC sequestration rates were compared using a quantile-quantile (Q-

249 Q) plot. First, the comparison was done via assessment of the Q–Q plots. Four sample datasets were used to construct Q-Q
250 plots to compare the distribution of ^{137}Cs - and ^{210}Pb -based OC sequestration against the 1:1 line.

251

252 The sample datasets included:

253

- 254 • D1, all suitable ^{137}Cs and ^{210}Pb profiles with OC sequestration rates estimated since 1954 ($n = 44$).
- 255 • D2, all suitable ^{137}Cs and ^{210}Pb profiles with OC sequestration rates estimated since 1963 ($n = 44$).
- 256 • D3, high-quality ^{137}Cs and ^{210}Pb profiles with OC sequestration rates estimated since 1954 ($n = 30$).
- 257 • D4, high-quality ^{137}Cs and ^{210}Pb profiles with OC sequestration rates estimated since 1963 ($n = 30$).

258

259 A Q-Q plot was calculated for each dataset. The x- and y- coordinates of a point in a Q-Q plot corresponded to the p^{th}
260 percentiles of the two OC sequestration rate estimates being compared in the plot. Here, $p = (k - 0.5) / n$, where n is the
261 sample size and $k = 1, \dots, n$ (Jain et al., 2007). The distribution of the points on the Q-Q plot was compared against the $y = x$
262 (1:1) line to assess whether the two OC sequestration rate estimates are similar. If the points were distributed in a straight
263 line and close to a 1:1 line, then it suggested that the two estimates came from the same distribution. In contrast, if the points
264 were not distributed in a straight line or deviated from the 1:1 line, then it suggested that the two estimates did not come
265 from the same distribution. The Q-Q plots were generated in Microsoft Excel (Microsoft 365, Version 2402, Redmond,
266 WA).

267

268 Since interpreting the Q-Q plot through a visual inspection can be subjective to human perception, we compared the ^{137}Cs -
269 and ^{210}Pb -based OC sequestration rate estimates using a distance sampling model. A distance sampling model captures how
270 the detectability of objects from the observer (walking along a straight line) decreases with the increase in the object-to-
271 observer distance. If the objects are closely distributed along the observer's path (i.e., if points of the Q-Q plot were closely
272 distributed along the 1:1 line), then the distribution of the distances is expected to be a half normal distribution. The Cramer-
273 von Mises test was used to estimate whether the distances (q_1, q_2, \dots, q_n) from the points to the 1:1 line were from a half-
274 normal distribution. Given a set of distance samples (q_1, q_2, \dots, q_n) and a detection function, the Cramer-von Mises test
275 builds a model that fits the distance sampling data to the detection function (for details on modelling, see Miller et al., 2019).
276 A half-normal key is commonly used as a detection function, corresponding to a half-normal distribution's shape.

277

278 The Cramer-von Mises test produced a p-value and Akaike's Information Criterion (AIC) as its test statistic. A p-value larger
279 than the significant level ($p = 0.05$) indicated that the likelihood of points being observed closer to the 1:1 line is high and

280 that the probability decreases as the distances increase. This provided evidence of the points being closely distributed along
281 the 1:1 line. The AIC was used to rank the distance sampling models, which are built by the Cramer-von Mises test, from
282 best to worst (e.g., Burnham and Anderson, 2003); a small AIC value indicates a good fit to the half-normal key and thus
283 provides evidence that the points are close to the 1:1 line (Miller et al., 2019). The distance sampling Cramer-von Mises test
284 was computed using the “distance” package in R version 4.0.3 (Miller and Clark-Wolfe, 2023; R Core Team, 2023).

285 **3 Results**

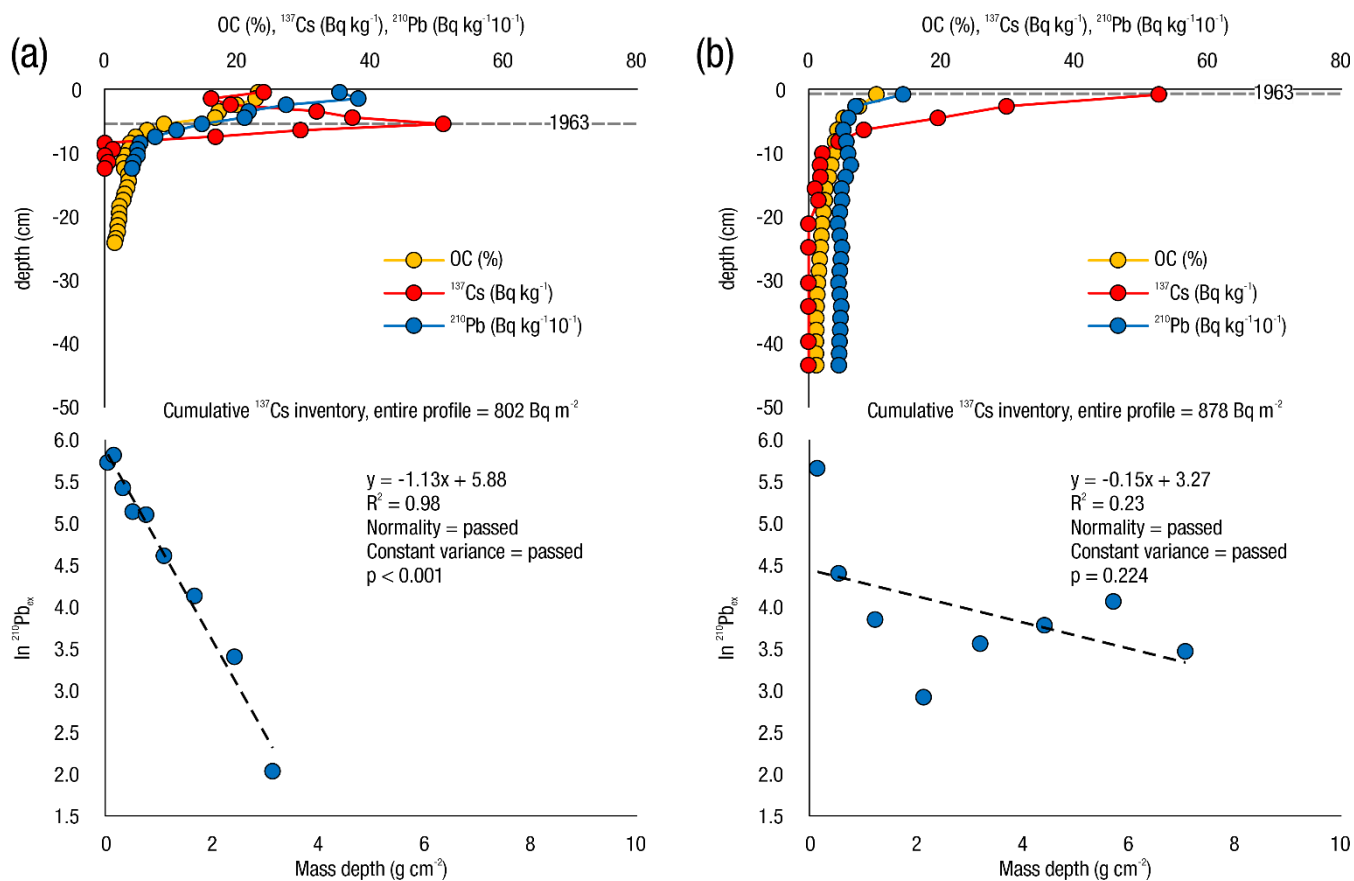
286 **3.1 High- and low-quality ^{137}Cs and ^{210}Pb profiles**

287 Of the 79 suitable ^{137}Cs profiles, 62 (78%) were classified as high-quality. Of the 62 high-quality ^{137}Cs profiles, 61% had
288 clear and distinct peaks, with a smooth rise and decline. In contrast, the remaining 39% had noise—either one-sided peaks or
289 disturbed peaks (e.g., Fig. 4). Of the 62 high-quality ^{137}Cs profiles, 4 (6.5%) were repositioned to capture the ^{137}Cs enriched
290 sediments post 1963 (e.g., ^{137}Cs profile of S-LO-I-W4-T2-CW-R2 in Supplementary Fig. 2a). In these profiles, which had a
291 cumulative ^{137}Cs inventory value $> 1,200 \text{ Bq m}^{-2}$, the depth that corresponded to ^{137}Cs cumulative inventory value of ~ 500
292 Bq m^{-2} was considered as the 1963 time-marker. The high total quantities of ^{137}Cs profile inventories can be attributed to
293 receiving ^{137}Cs enriched sediments from the surrounding landscape. Sediments that have undergone substantial preferential
294 detachment and entrainment on their pathway into a wetland can have very high concentrations of ^{137}Cs and, when
295 interlayered with sediments that are not so enriched, can generate multiple ^{137}Cs peaks in the sediment profile peaks after
296 1963. These observed multiple peaks are local and not regional, ruling out the association with Chernobyl and Fukushima
297 events. Two ^{137}Cs profiles were considered high-quality despite a cumulative ^{137}Cs inventory value $< 500 \text{ Bq m}^{-2}$ because the
298 1963 peak was clear, distinct, and elongated with two-to-three points on both sides of the peak (e.g., ^{137}Cs profile of M-OA-
299 I-W4-T2-CW-R2 in Supplementary Fig. 7b). One ^{137}Cs profile was considered high-quality despite showing marginal
300 quality to the set criteria in the decision framework, where the peak profile had good shape with several points on the
301 downside of the peak and one point on the other side and had a cumulative ^{137}Cs inventory value of 499 Bq m^{-2} . One ^{137}Cs
302 profile was classified as low-quality despite a cumulative ^{137}Cs inventory value $> 500 \text{ Bq m}^{-2}$ because the peak was highly
303 fluctuating and not discernible (e.g., ^{137}Cs profile of O-AL-I-W6-T1-CW-R1 in Supplementary Fig. 12b).

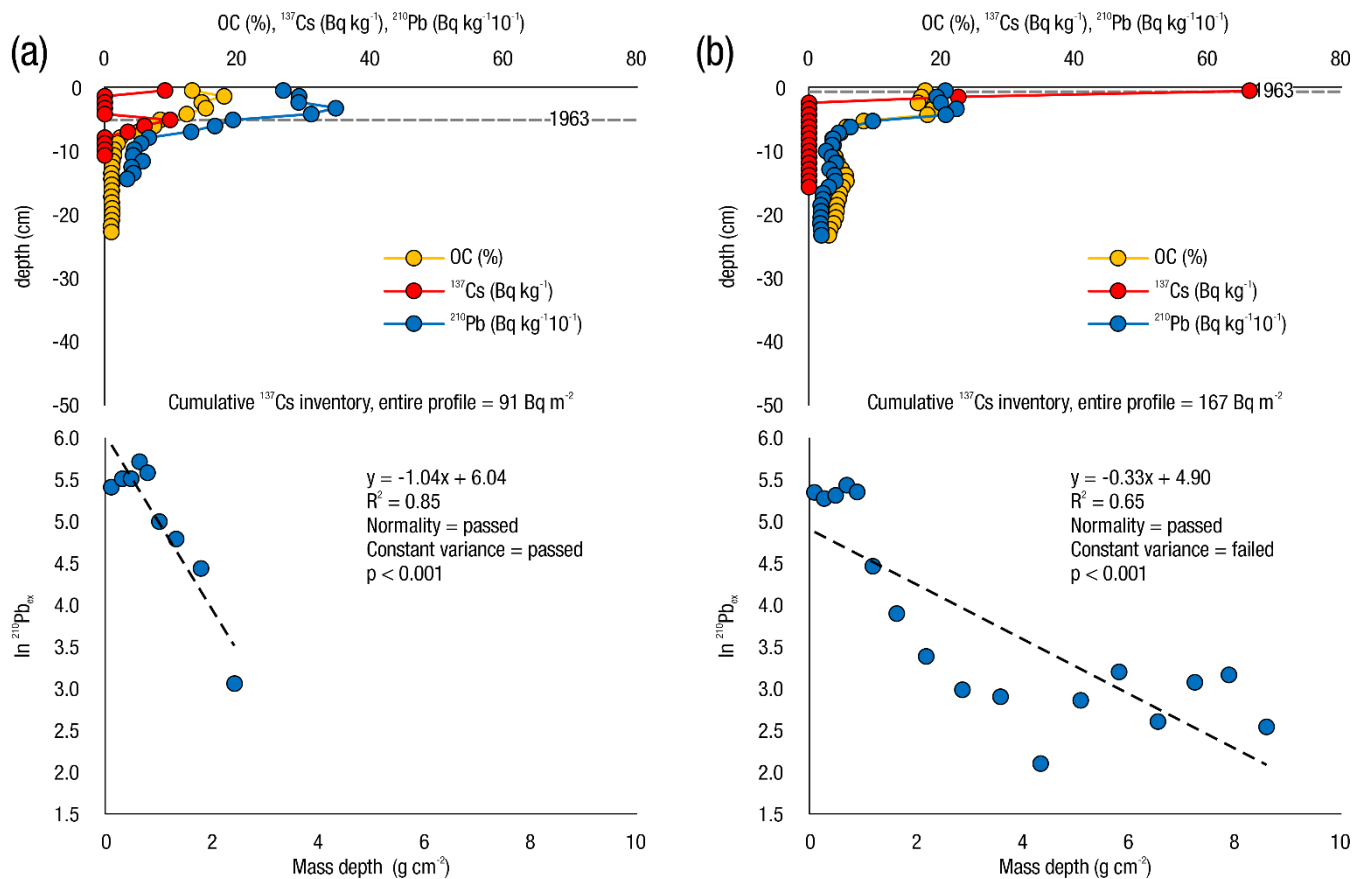
304
305 Of the 47 ^{210}Pb profiles, 40 (85%) were classified as high-quality.

306
307 There were 44 sediment cores with both ^{137}Cs and ^{210}Pb suitable profiles available. Of these, 30 were categorized as high-
308 quality ^{137}Cs and high-quality ^{210}Pb (Fig. 3a), six were categorized as high-quality ^{137}Cs and low-quality ^{210}Pb (Fig. 3b),

309 seven were classified as low-quality ^{137}Cs and high-quality ^{210}Pb (Fig. 4a), and one was categorized as low-quality ^{137}Cs and
 310 low-quality ^{210}Pb (Fig. 4b). (See Supplementary Figs. 1 to 12 for ^{137}Cs and ^{210}Pb profiles in all study wetlands.)
 311



312
 313 **Figure 3: Examples of ^{137}Cs and ^{210}Pb classifications showing OC (%), ^{137}Cs (Bq kg^{-1}), and ^{210}Pb (Bq kg^{-1}) depth profiles and plots**
 314 **of log-transformed $^{210}\text{Pb}_{\text{ex}}$ against mass depth (g cm^{-2}): (a) high-quality ^{137}Cs and high-quality ^{210}Pb (S-LO-I-W3-T1-CW-R1); (b)**
 315 **high-quality ^{137}Cs and low-quality ^{210}Pb (M-OA-I-W4-T3-CW-R3).**



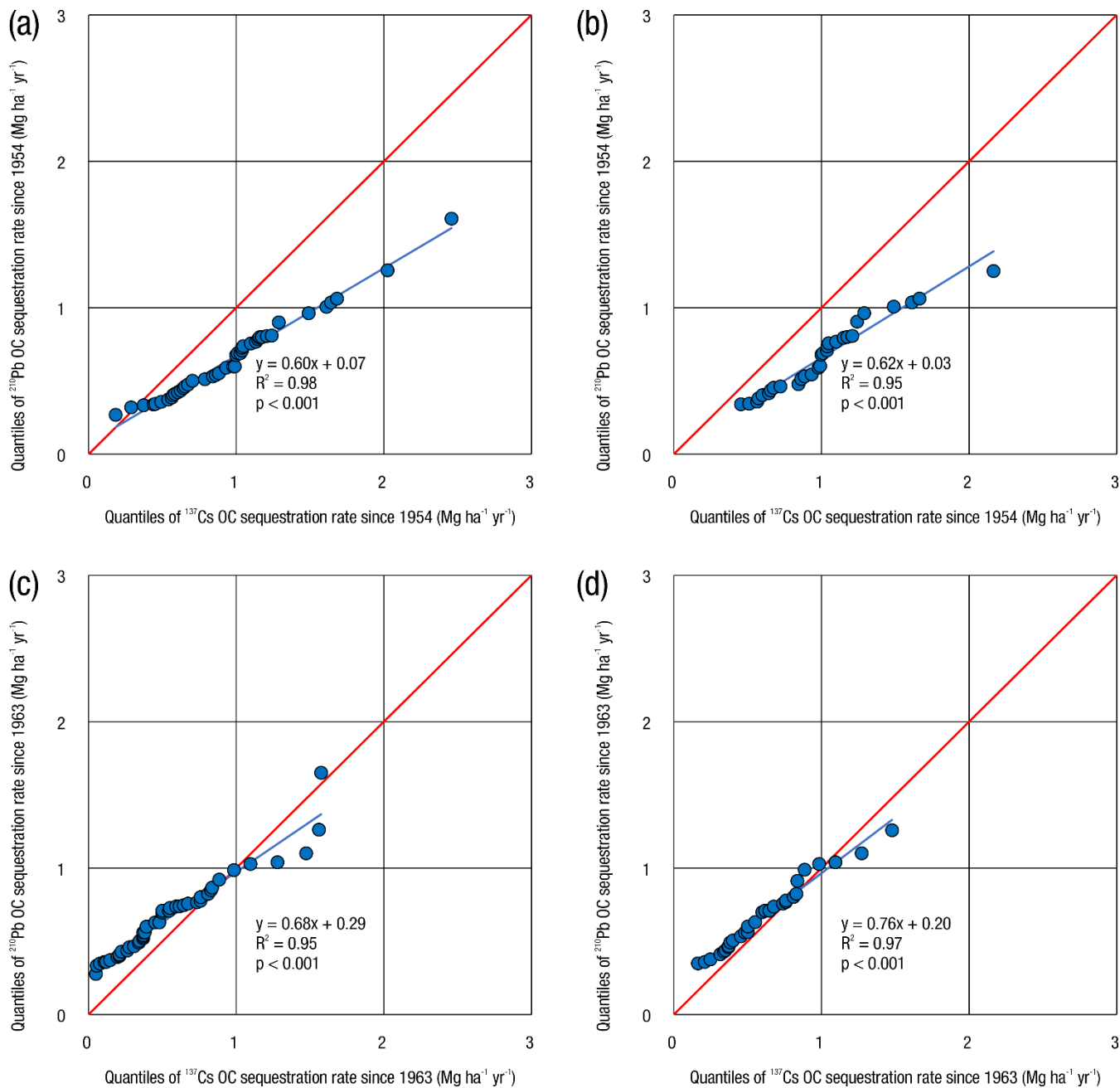
316

317 **Figure 4: Examples of ^{137}Cs and ^{210}Pb classifications showing OC (%), ^{137}Cs (Bq kg^{-1}), and ^{210}Pb (Bq kg^{-1}) depth profiles and plots of log-transformed $^{210}\text{Pb}_{\text{ex}}$ against mass depth (g cm^{-2}): (a) low-quality ^{137}Cs and high-quality ^{210}Pb (S-RO-I-W1-T3-CW-R3); and**
 318 **(b) low-quality ^{137}Cs and low-quality ^{210}Pb (S-RO-I-W6-T1-CW-R1).**
 319

320 3.2 ^{137}Cs vs. ^{210}Pb derived organic carbon sequestration rates

321

322 For each of the four datasets (D1-D4), the points on the Q-Q plot were distributed in a straight line, showing a linear
 323 relationship between the two estimates being compared ($R^2 > 0.95$, $p\text{-value} < 0.001$) (Fig. 5).



324

325

326

327

Figure 5: Q-Q plot of ^{137}Cs - vs. ^{210}Pb -based organic carbon (OC) sequestration rates using (a) all suitable ^{137}Cs and ^{210}Pb profiles estimated since 1954 (D1), (b) high-quality ^{137}Cs and ^{210}Pb profiles estimated since 1954 (D3), (c) all suitable ^{137}Cs and ^{210}Pb profiles estimated since 1963 (D2), and (d) high-quality ^{137}Cs and high-quality ^{210}Pb profiles estimated since 1963 (D4).

328 Visual inspection of the Q-Q plots showed that the points for D2 (i.e., all suitable ^{137}Cs and ^{210}Pb profiles using the 1963
 329 time-marker; Fig. 5c) and D4 (i.e., high-quality ^{137}Cs and ^{210}Pb profiles using the 1963 time-marker; Fig. 5d) were
 330 distributed more closely along the 1:1 line compared to that of D1 (i.e., all suitable ^{137}Cs and ^{210}Pb profiles using the 1954
 331 time-marker; Fig. 5a) and D3 (i.e., high-quality ^{137}Cs and ^{210}Pb profiles using the 1954 time-marker; Fig. 5b).

332
 333 An intercept closer to 0 and a slope closer to 1 indicated good alignment of the regression line to the 1:1 line. The slope (s)
 334 and intercept (i) of the regression lines were: $s = 0.60$, $i = 0.07$ for D1 (Fig. 5a); $s = 0.62$, $i = 0.03$ for D3 (Fig. 5b); $s = 0.68$, i
 335 $= 0.29$ for D2 (Fig. 5c); and $s = 0.76$, $i = 0.20$ for D4 (Fig. 5d). D2 and D4 had regression lines and slopes closer to the 1:1
 336 line but intercepts further from the origin than D1 and D3.

337
 338 The Cramer-von Mises test was used to build distance sampling models using the point-to-1:1-line distances computed from
 339 the Q-Q plots. Models built with the D4 dataset produced the best-fit model (i.e., $p\text{-value} > 0.05$, $\text{AIC} = -114$). Models built
 340 with the D1, D2, and D3 datasets had weaker $p\text{-values}$ ($p\text{-value} < 0.05$) and can be ranked based on lower AIC scores ($\text{AIC} =$
 341 -116 for D2, $\text{AIC} = -54$ for D1, and $\text{AIC} = -34$ for D3).

342 3.3 Sediment accumulation, organic carbon sequestration rates and stocks

343 The 30 sediment cores (68% of all the suitable ^{137}Cs and ^{210}Pb profiles) with high-quality ^{137}Cs and ^{210}Pb profiles were used
 344 to calculate mass or sediment accumulation rates, OC sequestration rates, and OC stocks (Table 2). OC sequestration rates
 345 based on ^{137}Cs and ^{210}Pb dating estimated since 1954 and 1963 of 44 suitable sediment cores (where both ^{137}Cs and ^{210}Pb
 346 profiles were available) are presented in Supplementary Table 2.

347 **Table 2: Sedimentation accumulation, OC stocks, and sequestration rates of undisturbed wetlands estimated using high-quality**
 348 **^{137}Cs and high-quality ^{210}Pb profiles.**

| Type of radiometric dating | ^{137}Cs | | ^{210}Pb | |
|--|-------------------|-------------|-------------------|-------------|
| | 1954 | 1963 | 1954 | 1963 |
| Time-marker | 1954 | 1963 | 1954 | 1963 |
| Range of accumulated sediment (Mg ha^{-1}) | 214-1,727 | 56-1,272 | 111-1,014 | 95-874 |
| Mean (standard deviation) stock of OC (Mg ha^{-1}) | 66 (29) | 35 (19) | 43 (18) | 38 (15) |
| Mean (standard deviation) rate of OC sequestration ($\text{Mg ha}^{-1} \text{ yr}^{-1}$) | 1.02 (0.44) | 0.63 (0.34) | 0.67 (0.27) | 0.68 (0.26) |

349

350 Based on the 1954 time-marker, the total sediment accumulation ranged from 214-1,727 Mg ha⁻¹ using ¹³⁷Cs dating and 111-
351 1,014 Mg ha⁻¹ using ²¹⁰Pb dating. In contrast, the total sediment accumulation based on the 1963 time-marker was lower,
352 ranging from 56-1272 Mg ha⁻¹ using ¹³⁷Cs and 95-874 Mg ha⁻¹ using ²¹⁰Pb dating.

353
354 The ¹³⁷Cs-derived mean OC sequestration rate was almost two times larger, at 1.02 Mg ha⁻¹ yr⁻¹ using the 1954 time marker
355 compared to 0.63 Mg ha⁻¹ yr⁻¹ using the 1963 time marker. The corresponding ¹³⁷Cs-based mean OC stocks were 66 Mg ha⁻¹
356 for 1954 and 35 Mg ha⁻¹ for 1963 (Table 2).

357
358 The ²¹⁰Pb-derived mean OC sequestration rate was similar at 0.67 Mg ha⁻¹ yr⁻¹ using the 1954 time-marker compared to 0.68
359 Mg ha⁻¹ yr⁻¹ using the 1963 time-marker. ²¹⁰Pb-based OC sequestration rates show minimal variation since they were
360 calculated using the same sedimentation rate. The corresponding mean OC stocks were 43 Mg ha⁻¹ for the 1954 time-marker
361 and 38 Mg ha⁻¹ for the 1963 time-marker, with a variable depth.

362
363 Figure 3 and Supplementary Figs. 1 to 12 present the depth distributions of ¹³⁷Cs and ²¹⁰Pb activity (along with the linear
364 plot of log-transformed ²¹⁰Pbex against mass depth in g cm⁻²) of all suitable profiles (n = 44) where both radioisotope
365 profiles are available.

366 **4 Discussion**

367 This study compared ¹³⁷Cs and ²¹⁰Pb dating for OC estimates in wetlands that were undisturbed (i.e., without direct impact
368 human activities) since both radioisotopes dating are known to provide reliable forecasts for recent OC sequestration rates
369 (i.e., post-1954, which coincides with the onset of ¹³⁷Cs atmospheric deposition) (Drexler et al., 2018; Creed et al., 2022).

370
371 This study highlights some advantages and disadvantages of using ¹³⁷Cs vs. ²¹⁰Pb dating. For example, the smaller number of
372 suitable ²¹⁰Pb profiles (47/90 = 52%) due to the lack of a complete decay profile (following the CFCS model as described in
373 Sanchez-Cabeza and Ruiz-Fernandez, 2012) indicates that ²¹⁰Pb dating is more prone to disturbance than ¹³⁷Cs (79/90 =
374 88%). For ¹³⁷Cs, even if the sediment core is disturbed, estimation of OC sequestration rates may be possible with careful
375 interpretation (e.g., see Fig. 2). The larger number of sediment cores using ¹³⁷Cs dating can be beneficial in accurately
376 representing the heterogeneity of OC sequestration rates as it provides a larger dataset (a 36% gain compared to ²¹⁰Pb).

377
378 Other advantages and disadvantages of ¹³⁷Cs vs. ²¹⁰Pb radioisotope dating are presented in Table 3. ¹³⁷Cs deposition was a
379 pulse that occurred in 1954 and 1963. At the 1963 peak, the activity declined with time because of two factors: (1) peak

380 natural radioactive decay, with the ^{137}Cs 30-year half-life reducing the peak size over time, and (2) peak attenuation due to
381 physical, chemical, or biological reasons (Drexler et al. 2018). The declining ^{137}Cs activity limits its applicability as a
382 radioisotope dating tool; however, recent studies have reported adequate ^{137}Cs reference inventories for Canadian landscapes
383 (Sutherland, 1991; Kachanoski and Von Bertoldi, 1996; Li et al., 2008; Mabit et al., 2014; Zarrinabadi et al., 2023). In
384 addition, the use of ^{137}Cs inventory for dating to complement the peak has addressed the potential inadequacies that could be
385 attributed to declining peak resolution with time. ^{137}Cs dating is advantageous for its simplicity in pre- and post-processing
386 of samples and the presence of additional time-markers in other regions (Breithaupt et al., 2018; Foucher et al., 2021). For
387 example, additional time-markers correspond to the 1986 Chernobyl nuclear plant accident and 2011 Fukushima accident.
388 However, their effect has yet to be recorded in North America due to the substantial distance from the source. Recognizing
389 that there may be regional or local variation in peaks, we used non-eroded ^{137}Cs reference sites to deal with regional
390 variation in deposition. We also used multiple sampling sites within wetlands to assess local variation in deposition. [Further,](#)
391 [we looked for evidence from Chernobyl and Fukushima nuclear events in our data but found none \(data not shown\).](#)
392

393 Further, we looked for evidence from Chernobyl and Fukushima nuclear events in our data but found none (data not shown).
394 ^{137}Cs dating is best suited for where the total OC is sequestered since a fixed time-marker (1954 onset or 1963 peak) or the
395 average OC sequestration rate is needed. In contrast, the atmospheric deposition of ^{210}Pb is continuous and, therefore, not
396 limited in its applicability as a radioisotope dating tool. ^{210}Pb dating is best suited for where variable OC sequestration rates
397 are needed over a more extended period (earlier than 1954). ^{210}Pb dating is advantageous because its calculations are based
398 on multiple points associated with progressive OC sequestration rates derived using a constant rate of supply model —
399 including the 1954 onset and 1963 peak of ^{137}Cs activity—improving the precision of the OC sequestration rates. This
400 precision enables estimating OC sequestration rates when wetlands are not undisturbed (history of drainage or at different
401 ages since restoration) and undisturbed (no history of drainage).

Table 3: The advantages and disadvantages of using ^{137}Cs and unsupported ^{210}Pb ($^{210}\text{Pb}_{\text{ex}}$) to estimate wetland organic carbon (OC) sequestration rates.

| Method of radiometric dating | ^{137}Cs | $^{210}\text{Pb}_{\text{ex}}$ |
|-------------------------------------|---|--|
| Advantages | <ul style="list-style-type: none"> • Calculations are based on single points representing the peak (1963) and onset (1954) of the fallout. There are additional time-markers for Europe (1986 due to the Chernobyl nuclear accident) and Japan (2011 due to Fukushima Daiichi nuclear accident). • Sedimentation peak may still be evident allowing estimation of OC sequestration rate even if parts of the sediment core are disturbed. • Sedimentation rate can be estimated using gamma detection, which is non-destructive, so sample can be re-analyzed or used for other analyses. • Less sample preparation time for gamma analysis. • After the ^{137}Cs activity is measured, post-processing of data is less challenging. | <ul style="list-style-type: none"> • Calculations are based on multiple points as there is continuous atmospheric deposition. • Sedimentation rate can be estimated using two reliable methods i.e., both alpha and gamma detection. • Less sample preparation time for gamma analysis compared to alpha. • Gamma analysis is non-destructive, so samples can be re-analyzed for other analyses compared to alpha. • Can run multiple samples at a time on a single detector in alpha method. |

| Method of radiometric dating | ^{137}Cs | $^{210}\text{Pb}_{\text{ex}}$ |
|------------------------------|---|--|
| Disadvantages | <ul style="list-style-type: none"> • Risk of mixing of restored and drained states when estimating OC sequestration rates due to specificity of the 1954 and 1963 time-markers (e.g., if drained and restored after 1963). • Declining atmospheric deposition and declining inventory due to radioactive decay (i.e., with no more nuclear testing, atmospheric deposition only comes from recent accidental releases from Chernobyl and Fukushima). • Sometimes the peak is not distinct. • Can be estimated using only one reliable method i.e., Gamma detection. • Can run only one sample at a time on a single detector. • Sensitive to vertical mobilization of sediments. • Sensitive to declining ^{137}Cs inventory due to radioactive decay. • Sensitive to changes in redox potential. • More sensitive to biological and chemical activity compared to ^{210}Pb (e.g., ^{137}Cs can be taken up by plants instead of sodium or potassium, and ^{137}Cs is soluble and therefore subject to mobility into solution then moving up and down the core). | <ul style="list-style-type: none"> • Requires full profile of ^{210}Pb to do the calculations, if the sediment core disturbed then it cannot be used to estimate OC sequestration rates. • Sensitive to vertical mobilization of sediments, but not as much as ^{137}Cs. • The alpha method is destructive, and therefore the sample is not available for re-use or re-analysis. • The alpha method requires extra precaution using hydrochloric acid for digesting, heating, spiking with ^{209}Po tracer (i.e., analysts come in direct contact with radioactive material ^{209}Po and hot acid). • The alpha method takes more time per sample (i.e., overnight digest followed by at least 48 h on the alpha counter), and is more labor intensive i.e., digest, engraving coins, plating, transferring into ensemble, etc.). • The alpha method requires more technical expertise for post processing of the data. • Uncertainty of $^{210}\text{Pb}_{\text{ex}}$ results derived from gamma analysis can be higher than alpha. |

405 **4.1 Challenges in interpreting the ¹³⁷Cs peak**

406 A potential weakness of ¹³⁷Cs radioisotope dating arises from the challenges in interpreting the disturbed 1963 peak. The
407 noise in the 1963 peak in wetlands on agricultural landscapes can be due to the redistribution of sediments since wetlands are
408 susceptible to receiving a large mass of sediments resulting from various erosional processes due to their positioning within
409 the landscape (Lobb et al., 2011; Zarrinabadi et al., 2023). Soil erosion resulting from wind, water, and tillage can lead to
410 higher or lower ¹³⁷Cs levels (Li et al., 2010; Foucher et al., 2021; Zarrinabadi et al., 2023) in wetlands in agricultural
411 landscapes. If ¹³⁷Cs enriched soil from the surrounding landscape gets deposited on top of the wetland's original soil layer, it
412 can increase the ¹³⁷Cs inventory value (Walling and Quine, 1991; Li et al., 2010). The magnitude of ¹³⁷Cs enrichment
413 depends on whether sediment comes from surface or sub-surface layers (Li et al., 2010; Lal, 2020). For example, if the
414 wetland receives ¹³⁷Cs enriched topsoil post-1963, the ¹³⁷Cs inventory would be higher than the ¹³⁷Cs depleted subsoil.
415

416 The screening of ¹³⁷Cs profiles (Fig. 2a) considered the redistribution of sediments within the landscape. It demonstrated that
417 the difficulty in disturbed ¹³⁷C profile interpretation can be reduced by investigating the cumulative ¹³⁷C inventory value. A
418 cutoff cumulative ¹³⁷Cs inventory value can help exclude questionable profiles. The range of ¹³⁷Cs reference inventory values
419 from previous erosion studies within the study area (e.g., Sutherland, 1991; Kachanoski and Von Bertoldi, 1996; Zarrinabadi
420 et al., 2023) can help in establishing and setting the cutoff cumulative ¹³⁷Cs inventory value. The mean ¹³⁷Cs reference
421 inventory values in the four provinces of Canada where our wetland sites are located were utilized in this instance. The mean
422 ¹³⁷Cs reference inventory value estimated to be 1,684 Bq m⁻² (coefficient of variation (CV) = 49%) for three AB wetland
423 sites (53° N and 113° W) (Zarrinabadi et al. 2023), 989 Bq m⁻² (CV = 20%) for seven SK wetland sites (51° N and 107° W)
424 (Sutherland, 1991), 1,008 Bq m⁻² (CV = 17.9%) for nine SK wetland sites (51° N and 104° W) (Sutherland, 1991), 1,430 Bq
425 m⁻² (CV = 8.6%) for five MB wetland sites (50° N and 100° W) (Zarrinabadi et al. 2023), 1,447 Bq m⁻² (CV = 8.8%) for
426 three ON wetland sites (43.3° N and 80.3° W) (Kachanoski and Von Bertoldi, 1996) and 1,534 Bq m⁻² (CV = 1.7%) for three
427 ON wetland sites (45.6° N and 74.8° W) (Kachanoski and Von Bertoldi, 1996). The ¹³⁷Cs reference inventory values were
428 decay-corrected to 2021 for comparability. The cutoff cumulative ¹³⁷Cs inventory value for this study was selected by
429 checking the minimum ¹³⁷Cs reference inventory value of the local region, i.e., 546 Bq m⁻² (using values reported in
430 Sutherland, 1991; Kachanoski and Von Bertoldi, 1996; Zarrinabadi et al. 2023). Hence, any ¹³⁷Cs inventory value less than
431 500 Bq m⁻² was considered questionable and low-quality. Additionally, > 75% of ¹³⁷C profiles had a cumulative ¹³⁷Cs
432 inventory value of > 500 Bq m⁻², indicating that our wetland sites' ¹³⁷Cs reference inventory value is most likely around 500
433 Bq m⁻².
434

435 Variations in the ^{137}Cs peak types (e.g., distinct, broadened, fluctuating, etc.) and in ^{137}Cs inventory values in this study
436 suggested that the ^{137}Cs profiles were impacted by various regional erosional processes in the surrounding agricultural
437 landscape. Recent evidence suggests that there may be an outward movement of sediment and ^{137}Cs from the center of the
438 wetlands to the riparian area (Zarrinabadi et al., 2023), suggesting that the base ^{137}Cs inventory value observed in the center
439 of wetlands from atmospheric deposition in the 1950s-1960s could be less than that of the non-eroded reference ^{137}Cs values
440 from the surrounding catchment. A ^{137}C inventory of a sediment core can further help assign the ^{137}Cs peak. For example, the
441 ^{137}Cs peak was repositioned in disturbed sediment cores with higher ^{137}Cs inventory, where the first discernable peak after
442 the sharp rise from the onset of ^{137}Cs activity and exceeding or around the reference value was assumed to be the original
443 ^{137}Cs peak. $^{239+240}\text{Pu}$ isotopes, like ^{137}Cs , are a product of nuclear testing and can be used to identify the peak of ^{137}Cs . Future
444 research will use $^{239+240}\text{Pu}$ to replace ^{137}Cs as ^{137}Cs levels diminish.

445 **4.2 Challenges in interpreting ^{137}Cs and ^{210}Pb profiles**

446 Mobilization of ^{137}Cs and ^{210}Pb in the sediment often occurs in wetlands. Vertical mixing of ^{137}Cs within sediments can be
447 caused by remobilization and redistribution by wind and water, ice movement and inversion, disturbance by animals, and
448 disturbance by humans that ditch and drain the wetlands till through the wetland when it is dry and let cattle access them for
449 water which causes disturbances to the bottom sediments (Robbins et al., 1977; Milan et al., 1995; Takahashi et al., 2015).
450 Vertical mixing affects the profile by attenuating the peak upward and downward (which we addressed using the ^{137}Cs
451 inventory value and not just the peak when assessing the profile). Horizontal mixing of ^{137}Cs dating within sediment occurs
452 by physical movement of sediments into or out of the wetland, causing uneven distribution of the OC content, where
453 accumulation may be high at the edges of open water of the wetland (Lobb et al., 2011; Zarrinabadi et al., 2023). This
454 heterogeneity can be caused by the horizontal focusing of sediments in sub-basins within a wetland, i.e., multiple center
455 points. Sampling multiple sediment cores from individual wetlands can help capture the heterogeneity within the wetland.
456 Suppose the ^{137}Cs activity of most of the sediment cores from a particular wetland is noisy with a higher inventory value
457 (e.g., ^{137}Cs profile of S-LO-I-W4-T2-CW-R2 in Supplementary Fig. 2a). In that case, the impact by erosional processes can
458 be deduced with higher certainty. The higher observed inventory value could result from the movement of enriched material
459 via erosion/lateral flow to the center of the wetland, increasing the number of ^{137}Cs . In this study, the assumption of no
460 substantial downward mixing of ^{137}Cs was supported by (1) sampling three cores from each wetland, (2) assessing the
461 sharpness of the rise of the peaks (a sharp rise means negligible mixing), (3) examining the cumulative ^{137}Cs inventory value
462 and validating against the known reference level, (4) classifying ^{137}Cs profiles, and (5) corroborating with ^{210}Pb dating.

463 4.3 ¹³⁷Cs vs. ²¹⁰Pb derived OC sequestration rates and stocks

464 ¹³⁷Cs radioisotope dating using the 1954 or 1963 time-markers gives reasonable estimates of OC sequestration rates as
465 compared to ²¹⁰Pb radioisotope dating. The ¹³⁷Cs-²¹⁰Pb Q-Q plot of the 1963 OC sequestration rates is closer to the 1:1-line,
466 suggesting compatibility between ¹³⁷Cs- and ²¹⁰Pb-based estimates (Fig. 5c and 5d). Conversely, the ¹³⁷Cs-²¹⁰Pb Q-Q plot of
467 the 1954 OC sequestration rates showed more deviation from the 1:1 line; ¹³⁷Cs-based OC sequestration rates were more
468 dispersed and were higher than the ²¹⁰Pb-based OC sequestration rates (Fig. 5a and 5b). The mean OC sequestration rates in
469 Table 2 further verify the comparability of OC sequestration rates using the 1963 time-marker (mean ¹³⁷Cs OC sequestration
470 rate is 0.63 Mg ha⁻¹ yr⁻¹ while mean ²¹⁰Pb OC sequestration rate is 0.68 Mg ha⁻¹ yr⁻¹). The dispersion using the 1954 time-
471 marker (mean ¹³⁷Cs OC sequestration rate is 1.02 Mg ha⁻¹ yr⁻¹ while mean ²¹⁰Pb OC sequestration rate is 0.67 Mg ha⁻¹ yr⁻¹).
472 Providing better sequestration rate estimates has consequences for estimating OC stocks with an improved degree of
473 accuracy, which may provide policymakers with better tools to make informed carbon management decisions supported with
474 data.

475
476 To put our findings into practice and in the broader OC sequestration perspective, we consider a scenario where two
477 independent studies were performed using ¹³⁷Cs and ²¹⁰Pb (with the CFCS model) at the exact locations. If the cores were
478 not selected based on the criteria we used to choose high-quality profiles, then these two studies' OC sequestration rate
479 estimates are likely to disagree. However, we know and have demonstrated through our findings that they are linearly
480 dependent, and the equation of our linear regression lines may be used to transform one estimate to the other. Consequently,
481 if the cores were selected based on our selection criteria, then one can expect the OC sequestration rate estimates to have
482 similar values, which alleviates the interpretation challenges of having two different estimates from two independent studies.
483 This observation may help with consistency when disagreements in estimates are observed. Another practical application of
484 our findings may be in data augmentation. For example, if we have ²¹⁰Pb data for a set of locations and ¹³⁷Cs data for other
485 locations, the linear regression equation could transform ²¹⁰Pb data to augment ¹³⁷Cs data, and vice versa. This can help data-
486 driven modelling approaches, whereas larger datasets help achieve robust modelling tools. Similarly, because OC stocks can
487 be derived from sequestration rates for specific years, estimates derived using one radioisotope can be used to estimate OC
488 from a dataset derived from another estimate, further contributing to the augmentation of the corresponding OC stock data.

489
490 Based on the results of this study, we recommend (1) using high-quality ¹³⁷Cs and ²¹⁰Pb profiles to estimate OC
491 sequestration rates, (2) interpreting ¹³⁷Cs profiles from agricultural landscapes carefully from the perspective of
492 redistribution of sediments, (3) using both ¹³⁷Cs and ²¹⁰Pb to compare and validate estimates if logistic approves. However,
493 in case where one had to choose between ¹³⁷Cs and ²¹⁰Pb we recommend (1) For ¹³⁷Cs: use 1963 time-markers to estimate
494 OC sequestration rates (compared to 1954) since it is found to be most comparable with ²¹⁰Pb dating techniques (CFCS

495 model), (2) For ^{210}Pb (CFCS model): OC sequestration rates from present to 1963 can be estimated with highest precision
496 since we corroborated the estimates with ^{137}Cs . However, we cannot comment on the precision of ^{210}Pb -based OC
497 sequestration rate estimation before 1963 based on the scope of this study.

498 **5 Conclusions**

499 Information regarding OC sequestration rates within temperate inland wetland soils is crucial for evaluating the potential of
500 these ecosystems to serve as natural climate solutions. Radiometric dating using ^{137}Cs and ^{210}Pb presents a valuable tool for
501 estimating the recent OC sequestration potential of wetlands. Notably, a robust 1:1 linear correlation has been observed
502 between ^{137}Cs - and ^{210}Pb -based OC sequestration rates in high-quality sediment profiles.

503
504 While estimations based on the onset of ^{137}Cs in 1954 or its peak in 1963 were reasonable, estimates anchored to the 1963
505 peak of ^{137}Cs exhibited closer alignment with those derived from ^{210}Pb data (using the CFCS model). These findings suggest
506 that estimates derived from ^{137}Cs and ^{210}Pb radioisotope dating methods are interchangeable and reasonably comparable
507 when utilizing the 1963 ^{137}Cs time-marker.

508
509 Combining ^{137}Cs and ^{210}Pb tracers provides a comprehensive assessment of sedimentation rates. While one tracer offers an
510 average sedimentation rate over 60 years, the other provides a temporal trend over the same period. This interchangeability
511 enables more thorough evaluations of the average sedimentation rate in wetlands, which is crucial for leveraging them as
512 natural climate solutions.

513 **Code and data availability.** The R code for the distance sampling modelling along with the data to run the code is available
514 at <https://doi.org/10.5281/zenodo.10951658>. The organic carbon (OC) sequestration rates data used to check the
515 comparability of the radioisotope profiles can be found in the Supplement. The radioisotope profiles used for screening are in
516 the paper and Supplement. The paper and Supplement present other relevant data to support our conclusion.

517

518 **Author contributions.** The authors' contributions are as follows: PM: methodology, field and lab analysis, statistical
519 analysis and modelling, writing; IFC: conceptualization, methodology, field and lab analysis, editing, supervision; CGT:
520 conceptualization, editing, supervision; EE: methodology, field and lab analysis, editing; and DAL: methodology, field and
521 lab analysis, editing.

522

523 **Competing interests.** The authors declare that they have no conflict of interest.

524

525 **Acknowledgements.** We acknowledge the support of the Natural Sciences and Engineering Research Council of Canada
526 (NSERC): Strategic Partnership Grant (STPGP 506809) to IFC, DAL, and CGT. Additional funding sources are the NSERC
527 Canadian Graduate Scholarship, Saskatchewan Innovation and Opportunity Scholarship, PhD Scholarship, School of
528 Environment and Sustainability, University of Saskatchewan, and Wanda Young Scholarship awarded to PM. We thank
529 Jacqueline Serran, Kevin Erratt, Oscar Senar, Ehsan Zarrinabadi, and many others for assisting in field sampling.

530 **References**

- 531 Andersen, T. J., Mikkelsen, O. A., Møller, A. L., and Pejrup, M.: Deposition and mixing depths on some European intertidal
532 mudflats based on ²¹⁰Pb and ¹³⁷Cs activities, *Continental Shelf Research*, 20(12-13), 1569-1591, doi:
533 10.1016/S0278-4343(00)00038-8, 2000.
- 534 Appleby, P. G. and Oldfield, F.: The calculation of lead-210 dates assuming a constant rate of supply of unsupported ²¹⁰Pb
535 to the sediment, *Catena*, 5(1), 1-8, doi:10.1016/S0341-8162(78)80002-2, 1978.
- 536 Appleby, P. G., and Oldfieldz, F.: The assessment of ²¹⁰Pb data from sites with varying sediment accumulation rates,
537 *Hydrobiologia*, 103, 29-35, doi:10.1007/BF00028424, 1983.
- 538 Bansal, S., Creed, I. F., Tangen, B. A., Bridgham, S. D., Desai, A. R., Krauss, K. W., Neubauer, S. C., Noe, G. B.,
539 Rosenberry, D. O., Trettin, C., Wickland, K. P., Allen, S. T., Arias-Ortiz, A., Armitage, A. R., Baldocchi, D.,
540 Banerjee, K., Bastviken, D., Berg, P., Bogard, M., Chow, A. T., Conner, W. H., Craft, C., Creamer, C., DelSontro,
541 T., Duberstein, J. A., Eagle, M., Fennessy, M. S., Finkelstein, S. A., Göckede, M., Grunwald, S., Halabisky, M.,
542 Herbert, E., Jahangir, M. M. R., Johnson, O. F., Jones, M. C., Kelleway, J. J., Knox, S., Kroeger, K. D., Kuehn, K.
543 A., Lobb, D., Loder A. L., Ma, S., Maher, D. T., McNicol, G., Meier, J., Middleton, B. A., Mills, C., Mistry, P.,
544 Mitra, A., Mobbian, C., Nahlik, A. M., Newman, S., O'Connell, J. L., Oikawa, P., Post van der Burg, M., Schutte,
545 C. A., Song, C., Stagg, C. L., Turner, J., Vargas, R., Waldrop, M. P., Wallin, M. B., Wang, Z. A., Ward, E. J.,
546 Willard, D. A., Yarwood, S., and Zhu X.: Practical guide to measuring wetland carbon pools and
547 fluxes, *Wetlands*, 43(8), 105, doi:10.1007/s13157-023-01722-2, 2023.
- 548 Bellucci, L. G., Frignani, M., Cochran, J. K., Albertazzi, S., Zaggia, L., Cecconi, G., and Hopkins, H.: ²¹⁰Pb and ¹³⁷Cs as
549 chronometers for salt marsh accretion in the Venice Lagoon—links to flooding frequency and climate change,
550 *Journal of Environmental Radioactivity*, 97(2-3), 85-102, doi:10.1016/j.jenvrad.2007.03.005, 2007.
- 551 Bernal, B. and Mitsch, W. J.: Comparing carbon sequestration in temperate freshwater wetland communities, *Global Change*
552 *Biology*, 18(5), 1636-1647, doi:10.1111/j.1365-2486.2011.02619.x, 2012.
- 553 Bernal, B. and Mitsch, W. J.: Carbon sequestration in two created riverine wetlands in the Midwestern United States. *Journal*
554 *of environmental quality*, 42(4), 1236-1244, doi:10.2134/jeq2012.0229, 2013.
- 555 Breithaupt, J. L., Smoak, J. M., Byrne, R. H., Waters, M. N., Moyer, R. P., and Sanders, C. J.: Avoiding timescale bias in
556 assessments of coastal wetland vertical change, *Limnology and Oceanography*, 63(S1), S477-S495,
557 doi:10.1002/lno.10783, 2018.
- 558 Bridgham, S. D., Megonigal, J. P., Keller, J. K., Bliss, N. B., and Trettin, C.: The carbon balance of North American
559 wetlands, *Wetlands*, 26(4), 889-916, doi:10.1672/0277-5212(2006)26[889:TCBONA]2.0.CO;2, 2006.

560 Burnham K. P. and Anderson D. R. (Eds.): Model Selection and Multimodel Inference: A Practical Information-Theoretic
561 Approach, Springer, doi:10.1007/b97636, 2003.

562 Craft, C. B. and Casey, W. P.: Sediment and nutrient accumulation in floodplain and depressional freshwater wetlands of
563 Georgia, USA. *Wetlands*, 20(2), 323-332, doi:10.1672/0277-5212(2000)020[0323:SANAIF]2.0.CO;2, 2000.

564 Craft, C. B. and Richardson, C. J.: Recent and long-term organic soil accretion and nutrient accumulation in the
565 Everglades, *Soil Science Society of America Journal*, 62(3), 834-843,
566 doi:10.2136/sssaj1998.03615995006200030042x, 1998.

567 Craft, C., Vymazal, J., and Kröpfelová, L.: Carbon sequestration and nutrient accumulation in floodplain and depressional
568 wetlands. *Ecological Engineering*, 114, 137-145, doi:10.1016/j.ecoleng.2017.06.034, 2018.

569 Creed, I. F., Badiou, P., Enanga, E., Lobb, D. A., Pattison-Williams, J. K., Lloyd-Smith, P., and Gloutney, M.: Can
570 restoration of freshwater mineral soil wetlands deliver nature-based climate solutions to agricultural landscapes?,
571 *Frontiers in Ecology and Evolution*, 10, 932415, doi:10.3389/fevo.2022.932415, 2022.

572 DeLaune, R. D., Jugsujinda, A., Peterson, G. W., and Patrick Jr, W. H.: Impact of Mississippi River freshwater
573 reintroduction on enhancing marsh accretionary processes in a Louisiana estuary, *Estuarine, Coastal and Shelf
574 Science*, 58(3), 653-662, doi:10.1016/S0272-7714(03)00177-X, 2003.

575 Drexler, J. Z., Fuller, C. C., and Archfield, S.: The approaching obsolescence of ¹³⁷Cs dating of wetland soils in North
576 America, *Quaternary Science Reviews*, 199, 83-96, doi:10.1016/j.quascirev.2018.08.028, 2018.

577 Environment and Climate Change Canada (ECCC): Canadian Environmental Sustainability Indicators: Extent of Canada's
578 Wetlands, ECCC, Gatineau, Quebec, www.ec.gc.ca/indicateurs-indicators/default.asp?lang=en&n=69E2D25B-1,
579 last access: 10 July 2024, 2016.

580 Foucher, A., Chaboche, P. A., Sabatier, P., and Evrard, O.: A worldwide meta-analysis (1977–2020) of sediment core dating
581 using fallout radionuclides including ¹³⁷Cs and ²¹⁰Pb xs, *Earth System Science Data Discussions*, 2021, 1-61,
582 doi:10.5194/essd-13-4951-2021, 2021.

583 Hambäck, P. A., Dawson, L., Geranmayeh, P., Jarsjö, J., Kačergytė, I., Peacock, M., Collentine, D., Destouni, G., Futter,
584 M., Hugelius, G., Hedman, S., Jonsson, S., Klatt, B. K., Lindström, A., Nilsson, J. E., Pärt, T., Schneider, L. D.,
585 Strand, J. A., Urrutia-Cordero, P., Åhlén, D., Åhlén, I., and Blicharska, M.: Tradeoffs and synergies in wetland
586 multifunctionality: A scaling issue. *Science of the Total Environment*, 862, 160746,
587 doi:10.1016/j.scitotenv.2022.160746, 2023.

588 Hoogsteen, M. J., Lantinga, E. A., Bakker, E. J., Groot, J. C., and Tittonell, P. A.: Estimating soil organic carbon through
589 loss on ignition: effects of ignition conditions and structural water loss, *European Journal of soil science*, 66(2),
590 320-328, doi:10.1111/ejss.12224, 2015.

591 Jain, J. L., Mohanty, S. G., and Böhm, W.: *A Course on Queueing Models*, Chapman and Hall/CRC, doi:10.1201/b15892,
592 2007.

593 Kachanoski, R. G. and Von Bertoldi, P.: *Monitoring soil loss and redistribution using 137 Cs*, COESA Report No.
594 RES/MON-008/96, Green Plan Research Sub-program, Agriculture and Agri-food Canada, London, Ontario, 1996.

595 Klaminder, J., Appleby, P., Crook, P., and Renberg, I.: Post-deposition diffusion of 137Cs in lake sediment: Implications for
596 radiocaesium dating, *Sedimentology*, 59: 2259–2267, doi:10.1111/j.1365-3091.2012.01343.x, 2012.

597 Kamula, C. M., Kuzyk, Z. Z. A., Lobb, D. A., and Macdonald, R. W.: Sources and accumulation of sediment and particulate
598 organic carbon in a subarctic fjord estuary: 210Pb, 137Cs, and $\delta^{13}C$ records from Lake Melville,
599 Labrador, *Canadian Journal of Earth Sciences*, 54(9), 993-1006, doi:10.1139/cjes-2016-0167, 2017.

600 Kolthoff, I. M. and Sandell, E. B.: *Textbook of quantitative inorganic analysis*, The Macmillan Company,
601 doi:10.1002/sce.3730380480, 1952.

602 Lal, R. (2020). Soil erosion and gaseous emissions. *Applied Sciences*, 10, 2784, doi:10.3390/app10082784, 2020.

603 Li, S., Lobb, D. A., Lindstrom, M. J., and Farenhorst, A.: Tillage and water erosion on different landscapes in the northern
604 North American Great Plains evaluated using 137Cs technique and soil erosion models, *Catena*, 70(3), 493-505,
605 doi:10.1016/j.catena.2006.12.003, 2007.

606 Li, S., Lobb, D. A., Lindstrom, M. J., and Farenhorst, A.: Patterns of water and tillage erosion on topographically complex
607 landscapes in the North American Great Plains, *journal of soil and water conservation*, 63(1), 37-46,
608 doi:10.2489/jswc.63.1.37, 2008.

609 Li, S., Lobb, D. A., Tiessen, K. H., and McConkey, B. G.: Selecting and applying cesium-137 conversion models to estimate
610 soil erosion rates in cultivated fields, *Journal of environmental quality*, 39(1), 204-219, 2010.
611 doi:10.2134/jeq2009.0144, 2010.

612 Lobb, D. A.: Understanding and managing the causes of soil variability, *Journal of Soil and Water Conservation*, 66(6),
613 175A-179A, doi:10.2489/jswc.66.6.175A, 2011.

614 Loder, A. L., and Finkelstein, S. A.: Carbon accumulation in freshwater marsh soils: A synthesis for temperate North
615 America, *Wetlands*, 40(5), 1173-1187, doi:10.1007/s13157-019-01264-6, 2020.

616 Mabit L., Kieth, S. C., Dornhofer, P., Toloza, A., Benmansour, M., Bernard, C., Fulajtar, E., and Walling D. E.: 137Cs: A
617 widely used and validated medium term soil tracer, *Guidelines for Using Fallout Radionuclides to Assess Erosion*

618 and Effectiveness of Soil Conservation Strategies, IAEA-TECDOC-1741, Vienna, doi:10.13140/2.1.2586.1122,
619 2014.

620 Milan, C. S., Swenson, E. M., Turner, R. E., and Lee, J. M.: Assessment of the method for estimating sediment accumulation
621 rates: Louisiana salt marshes, *Journal of Coastal Research*, 296-307, <https://www.jstor.org/stable/4298341>, 1995.

622 Miller, D. L. and Clark-Wolfe, T. J.: Package “Distance”, <https://cran.r-project.org/web/packages/Distance/Distance.pdf>,
623 2023.

624 Miller, D. L., Rexstad, E., Thomas, L., Marshall, L., and Laake, J. L.: Distance sampling in R. *Journal of Statistical*
625 *Software*, 89(1), 1–28, doi:10.18637/jss.v089.i01, 2019.

626 Nahlik, A. M. and Fennessy, M. S.: Carbon storage in US wetlands. *Nature Communications*, 7(1), 1-9,
627 doi:10.1038/ncomms13835, 2016.

628 Owens, P. N. and Walling, D. E.: Spatial variability of caesium-137 inventories at reference sites: an example from two
629 contrasting sites in England and Zimbabwe, *Applied Radiation and Isotopes*, 47(7), 699-707, doi:10.1016/0969-
630 8043(96)00015-2, 1996.

631 Pennington, W., Tutin, T. G., Cambray, R. S., and Fisher, E. M.: Observations on lake sediments using fallout 137Cs as a
632 tracer, *Nature*, 242(5396), 324-326, doi:10.1038/242324a0, 1973.

633 Pribyl, D. W.: A critical review of the conventional SOC to SOM conversion factor, *Geoderma*, 156(3-4), 75-83,
634 doi:10.1016/j.geoderma.2010.02.003, 2010.

635 R Core Team: R: A language and environment for statistical computing, R Foundation for Statistical Computing, Vienna,
636 Austria, <https://www.R-project.org/>, 2023.

637 Ritchie, J. C. and McHenry, J. R.: Application of radioactive fallout cesium-137 for measuring soil erosion and sediment
638 accumulation rates and patterns: A review. *Journal of environmental quality*, 19(2), 215-233,
639 doi:10.2134/jeq1990.00472425001900020006x, 1990.

640 Robbins, J.A., Krezoski, J.R. and Mozley, S.C.: Radioactivity in sediments of the Great Lakes: post-depositional
641 redistribution by deposit-feeding organisms, *Earth Planet. Sci. Lett.*, 36, 325–333, doi: 10.1016/0012-
642 821X(77)90217-5, 1977.

643 Sanchez-Cabeza, J. A. and Ruiz-Fernández, A. C.: 210Pb sediment radiochronology: an integrated formulation and
644 classification of dating models, *Geochimica et Cosmochimica Acta*, 82, 183-200, doi:10.1016/j.gca.2010.12.024,
645 2012.

646 Sutherland, R. A.: Examination of caesium-137 areal activities in control (uneroded) locations, *Soil technology*, 4(1), 33-50,
647 doi:10.1016/0933-3630(91)90038-O, 1991.

648 Takahashi, J., Tamura, K., Suda, T., Matsumura, R., and Onda, Y.: Vertical distribution and temporal changes of ^{137}Cs in
649 soil profiles under various land uses after the Fukushima Dai-ichi Nuclear Power Plant accident, *Journal of*
650 *environmental radioactivity*, 139, 351-361, doi:10.1016/j.jenvrad.2014.07.004, 2015.

651 United Nations Scientific Committee on the Effects of Atomic Radiation (UNSCEAR): Sources and Effects of Ionizing
652 Radiation, V1, United Nations, New York, doi:10.18356/49c437f9-en, 2000.

653 Villa, J. A. and Bernal, B.: Carbon sequestration in wetlands, from science to practice: An overview of the biogeochemical
654 process, measurement methods, and policy framework, *Ecological Engineering*, 114, 115-128,
655 doi:10.1016/j.ecoleng.2017.06.037, 2018.

656 Walling, D. E. and He, Q.: Using fallout lead-210 measurements to estimate soil erosion on cultivated land. *Soil Science*
657 *Society of America Journal*, 63(5), 1404-1412, doi:10.2136/sssaj1999.6351404x, 1999.

658 Walling, D. E. and Quine, T. A.: Use of ^{137}Cs measurements to investigate soil erosion on arable fields in the UK: potential
659 applications and limitations, *Journal of Soil Science*, 42(1), 147-165, doi:10.1111/j.1365-2389.1991.tb00099.x,
660 1991.

661 Zaborska, A., Carroll, J., Papucci, C., and Pempkowiak, J.: Intercomparison of alpha and gamma spectrometry techniques
662 used in ^{210}Pb geochronology. *Journal of environmental radioactivity*, 93(1), 38-50,
663 doi:10.1016/j.jenvrad.2006.11.007, 2007.

664 Zarrinabadi, E., Lobb, D. A., Enanga, E., Badiou, P., and Creed, I. F.: Agricultural activities lead to sediment infilling of
665 wetlandscapes in the Canadian Prairies: Assessment of soil erosion and sedimentation fluxes, *Geoderma*, 436,
666 116525, doi:10.1016/j.geoderma.2023.116525, 2023.

667 Zhang, F., Wang, J., Baskaran, M., Zhong, Q., Wang, Y., Paatero, J., and Du, J.: A global dataset of atmospheric ^7Be and
668 ^{210}Pb measurements: annual air concentration and depositional flux, *Earth System Science Data*, 13(6), 2963-
669 2994, doi:10.5194/essd-13-2963-2021, 2021.